Strong Localized Perturbations: Theory and Applications

M. J. WARD

Michael J. Ward; Department of Mathematics, University of British Columbia, Vancouver, British Columbia, V6T 1Z2, Canada,

(*July 2015: AARMS Summer School*)

1 Localized Spot Patterns in an RD System

Localized spatio-temporal patterns consisting of spots or clusters of spots have been observed in many physical and chemical experiments. Such localized patterns can exhibit a variety of dynamical behaviors and instabilities including slow spot drift, temporal oscillations of spots, spot annihilation, and spot self-replication. Physical experiments where some of this phenomena has been observed include the ferrocyanide-iodate-sulphite reaction (cf. [**3**]), the chloride-dioxide-malonic acid reaction (cf. [**1**]), and certain semiconductor gas discharge systems.

Numerical simulations of certain singularly perturbed two-component reaction-diffusion systems with very simple kinetics, such as the Gray-Scott model, have shown the occurrence of very complex spatio-temporal localized patterns consisting of either spots, stripes, or space-filling curves in a two-dimensional domain (cf. [**4**]). Some of these reduced two-component reaction-diffusion systems model, at least qualitatively, the more complex chemically interacting systems of the experimental studies of [**3**] and [**1**]. A survey of experimental and theoretical studies, through reaction-diffusion modeling, of localized spot patterns in various physical or chemical contexts is given in [**5**].

Mathematically, a spot pattern for a reaction-diffusion system in a multi-dimensional domain Ω is a spatial pattern where at least one of the solution components is highly localized near certain discrete points in Ω that can evolve dynamically in time. For certain singularly perturbed two-component reaction-diffusion models in one space dimension, such as the Gray-Scott and Gierer-Meinhardt models, there has been considerable analytical progress in understanding both the dynamics and the various types of instabilities of spike patterns, including self-replicating instabilities. In contrast, in a two-dimensional spatial domain there are relatively few studies characterizing spot dynamics and stability. For a detailed literature survey, see [**2**].

In this section we study a class of nonlinear reaction-diffusion problems with localized spot patterns in a two-dimensional domain, An example of such a problem is the Schnakenburg reaction-diffusion model, studied in [**2**], formulated as

$$v_t = \varepsilon^2 \triangle v - v + uv^2\,, \qquad \varepsilon^2 u_t = D\triangle u + a - \varepsilon^{-2} uv^2\,, \quad x\in\Omega\,; \qquad \partial_n u = \partial_n v = 0\,, \quad x\in\partial\Omega\,. \tag{1.1}$$

Here $0<\varepsilon\ll 1$, $D>0$, and $a>0$, are parameters. Before beginning our analysis we will recall two simple results that we will use below.

Result 1: Let $y\in\mathbb{R}^2$ and assume that $f(y)\to 0$ sufficiently rapidly as $|y|\to\infty$. Then, in the limit $\epsilon\to 0$, and in the

sense of distributions we have

$$\varepsilon^{-2} f\left(\frac{x-x_0}{\varepsilon}\right) \to \left(\int_{\mathbb{R}^2} f(y)\,dy\right)\,\delta(x-x_0)\,. \tag{1.2}$$

Moroever, if $f(y)=f(|y|)$ and so is radially symmetric, then

$$\varepsilon^{-2} f\left(\frac{x-x_0}{\varepsilon}\right) \to 2\pi\left(\int_0^{\infty} \rho f(\rho)\,d\rho\right)\,\delta(x-x_0)\,. \tag{1.3}$$

provided that this integral is finite.

Result 2: Let Δ_ρ be the radially symmetric part of the Laplacian in 2-D, so that $\Delta_\rho \equiv \partial_{\rho\rho}+\rho^{-1}\partial_\rho$. Then, for $\rho\to\infty$, the solution to

$$\Delta_\rho v = f(\rho) \tag{1.4}$$

on $0<\rho<\infty$ has the far-field behavior

$$v \sim \left(\int_0^{\infty} \xi f(\xi)\,d\xi\right)\log\rho + O(1)\,, \quad \text{as} \quad \rho\to\infty\,, \tag{1.5}$$

provided that this integral is finite.

We now construct a quasi steady-state solution to (1.1) with K localized spots. Such a solution is characterized by the concentration of v as $\varepsilon\to 0$ to the vicinity of K distinct locations $x_1,\ldots,x_N$ in Ω. We assume that the distance between any two spots is $\mathcal{O}(1)$ as $\varepsilon\to 0$. In the inner region near the j^{th} spot we introduce the new variables

$$u = \frac{1}{\sqrt{D}}\,\mathcal{U}_j\,, \qquad v=\sqrt{D}\mathcal{V}_j\,, \qquad y=\varepsilon^{-1}(x-x_j)\,. \tag{1.6}$$

In the inner region, we look for a leading-order radially symmetric solution of the form $\mathcal{U}_j\sim U_j(\rho)$ and $\mathcal{V}_j\sim V_j(\rho)$ with $\rho=|y|$. Upon substituting this expansion into (1.1), and neglecting the term $\varepsilon^2 a$, we obtain to leading order that, for each $j=1,\ldots,K$, U_j and V_j

$$V_j''+\frac{1}{\rho}V_j'-V_j+U_jV_j^2=0\,; \quad U_j''+\frac{1}{\rho}U_j'-U_jV_j^2=0\,, \quad 0<\rho<\infty\,, \tag{1.7 a}$$

$$U_j'(0)=V_j'(0)=0\,; \quad V_j\to 0\,, \quad U_j\sim S_j\log\rho+\chi(S_j) \quad \text{as} \quad \rho\to\infty\,. \tag{1.7 b}$$

Here the primes denote derivatives in ρ. The local variable V_j decays exponentially as $\rho\to\infty$. In contrast, the far-field logarithmic behavior for U_j in (1.7 b) is similar to that for the case where the inner problem is Laplace's equation. We emphasize that the nonlinear function $\chi=\chi(S_j)$ in (1.7 b) must be computed numerically from the solution to (1.7) as a function of the source strength $S_j>0$. This function together with the numerically computed solutions are shown in Fig. 1. The nonlinear core problem (1.7) is the one that replaces the logarithmic capacitance problem for the linear problems with small traps considered in the previous lectures.

Next, we determine the source strengths $S_1,\ldots,S_K$ by matching the far-field behavior of U_j to an outer solution for u valid away from $\mathcal{O}(\varepsilon)$ distances from x_j. Firstly, upon writing the far-field condition for U_j in (1.7 b) in terms of outer variables, we obtain from the matching condition that the outer solution for u must have the local behavior

$$u\sim\frac{1}{\sqrt{D}}\left[S_j\log|x-x_j|+\frac{S_j}{\nu}+\chi(S_j)\right]\,, \quad x\to x_j\,, \tag{1.8}$$

for $j=1,\ldots,N$, where $\nu\equiv -1/\log\varepsilon$. Secondly, in the outer region, v is exponentially small, and from (1.6) and

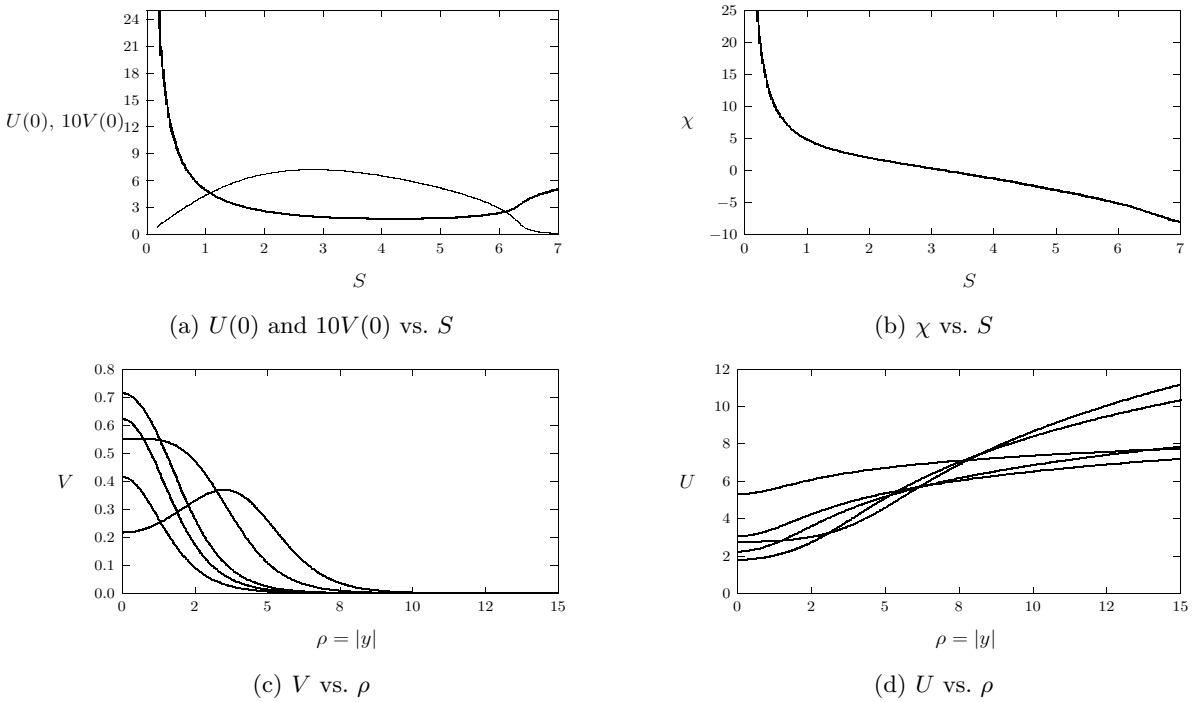

(a) $U(0)$ and $10V(0)$ vs. S

(b) χ vs. S

(c) V vs. ρ

(d) U vs. ρ

FIGURE 1. Numerical results computed from the core problem (1.7). Top left: $U(0)$ (heavy solid curve) and $10V(0)$ (solid curve) vs. S. Top right: χ vs. S. Bottom Row: $V(\rho)$ (left) and $U(\rho)$ (right) for $S = 0.94$, $S = 1.68$, $S = 2.44$, $S = 4.79$, and $S = 6.19$. The specific labels of these curves correspond to the values of $U(0)$ and $10V(0)$ in the top right figure. Notice that the profile for V has a volcano shape when $S > S_v \approx 4.78$.

(1.7 *b*) we get upon using Result 1 and Result 2 in (1.3) and (1.5) that

$$\varepsilon^{-2}uv^2 \to \frac{2\pi\sqrt{D}}{\varepsilon^2}\left(\varepsilon^2\int_0^\infty \rho U_j V_j^2\, d\rho\right)\delta(x-x_j) = 2\pi\sqrt{D}S_j\delta(x-x_j)\,. \tag{1.9}$$

Therefore, from (1.1), the outer steady-state solution for u satisfies

$$\Delta u = -\frac{a}{D} + \frac{2\pi}{\sqrt{D}}\sum_{j=1}^{K} S_j\,\delta(x-x_j)\,, \quad x\in\Omega\,; \qquad \partial_n u = 0\,, \quad x\in\partial\Omega\,, \tag{1.10 a}$$

$$u \sim \frac{1}{\sqrt{D}}\left[S_j\log|x-x_j| + \chi(S_j) + \frac{S_j}{\nu}\right] \quad \text{as} \quad x\to x_j\,, \quad j=1,\ldots,K\,, \tag{1.10 b}$$

where $\nu \equiv -1/\log\varepsilon$. We again observe that the singularity behavior in (1.10 *b*) specifies both the singular and regular parts of a Coulomb singularity. As such, each singularity behavior provides one equation for the determination of an algebraic system for the source strengths $S_1,\ldots,S_K$.

To solve this problem, we first note that the Divergence theorem enforces that $2\pi\sum_{j=1}^K S_j = a|\Omega|/\sqrt{D}$, where $|\Omega|$ is the area of Ω. The solution to (1.10) then can be represented in terms of the Neumann Green's function G, satisfying

$$\triangle G = \frac{1}{|\Omega|} - \delta(x-\xi)\,, \quad x\in\Omega\,; \quad \partial_n G = 0\,, \quad x\in\partial\Omega\,, \tag{1.11 a}$$

$$G(x;\xi) \sim -\frac{1}{2\pi}\log|x-\xi| + R(\xi) + o(1)\,, \quad \text{as} \quad x\to\xi\,; \quad \int_\Omega G(x;\xi)\,dx = 0\,. \tag{1.11 b}$$

Below when we study the dynamics of spots, we will need the next term in the local behavior of G as $x\to\xi$. This

more refined behavior is given by

$$G(x;\xi) \sim -\frac{1}{2\pi}\log|x-\xi| + R(\xi) + \nabla_x R|_{x=\xi}\cdot(x-\xi) + \cdots, \quad \text{as} \quad x\to\xi\,; \quad \int_\Omega G(x;\xi)\,dx = 0\,. \tag{1.12}$$

In terms of G, the solution for u is

$$u(x) = -\frac{2\pi}{\sqrt{D}}\left(\sum_{i=1}^{K} S_i G(x;x_i) + \chi\right). \tag{1.13}$$

Here χ is a constant to be found. By expanding (1.13) as $x\to x_j$, and comparing the resulting expression with the required singularity behavior in (1.10 b), we obtain for each $j=1,\dots,K$ that

$$S_j\log|x-x_j| - 2\pi S_j R(x_j) - 2\pi\chi - 2\pi\sum_{\substack{i=1\\ i\neq j}}^{K} S_i G(x_j;x_i) \sim S_j\log|x-x_j| + \chi(S_j) + \frac{S_j}{\nu}\,. \tag{1.14}$$

These matching conditions gives K equations relating $S_1,\dots,S_K$ and χ. We summarize our construction as follows:

Principal Result: *For given spot locations x_j for $j=1,\dots,K$, let S_j for $j=1,\dots,K$ and χ satisfy the nonlinear algebraic system (NAS)*

$$S_j + 2\pi\nu\left(S_j R_j + \sum_{\substack{i=1\\ i\neq j}}^{K} S_i G_{ji}\right) + \nu\chi(S_j) = -2\pi\nu\chi\,; \qquad \sum_{j=1}^{K} S_j = \frac{a|\Omega|}{2\pi\sqrt{D}}\,. \tag{1.15}$$

Here $\nu \equiv -1/\log\varepsilon$ with $G_{ji}\equiv G(x_j;x_i)$ and $R_j\equiv R(x_j)$, where G is the Neumann Green's function of (1.11) with regular part R. The nonlinear term $\chi(S_j)$ in (1.15) is as given in (1.7 b). Then, for $\varepsilon\to 0$, the outer solution for a K-spot quasi steady-state solution of (1.1) is given by (1.13), and the leading-order inner solutions are given by $u\sim D^{-1/2}U_j$ and $v\sim\sqrt{D}V_j$, where U_j and V_j is the solution to the core problem (1.7).

We emphasize that the system (1.15) contains all of the logarithmic correction terms of order $\mathcal{O}(\nu^k)$ for any k that are required in the construction of the quasi steady-state solution. Hence, we say that (1.15) has 'summed' all of the logarithmic terms in powers of ν for the source strengths $S_1,\dots,S_K$. The key difference here between this nonlinear problem and the linear problem for the MFPT considered in the previous lecture is that the source strengths now satisfy a nonlinear algebraic system of equations.

It is convenient to write (1.15) in matrix form as

$$(I + 2\pi\nu\mathcal{G})\,S_v + \nu\chi_v = -2\pi\nu u_c\boldsymbol{e}\,; \qquad \boldsymbol{e}^t S_v = \frac{a|\Omega|}{2\pi\sqrt{D}}\,. \tag{1.16}$$

Here I is the identity matrix, $\mathcal{G}$ is the Green's matrix, and the vectors S_v, χ_v, and $\boldsymbol{e}$, are defined by

$$\mathcal{G}\equiv\begin{pmatrix} R_{1,1} & G_{1,2} & \cdots & G_{1,K}\\ G_{2,1} & \ddots & \ddots & \vdots\\ \vdots & \ddots & \ddots & G_{K-1,K}\\ G_{K,1} & \cdots & G_{K,K-1} & R_{K,K}\end{pmatrix}, \qquad S_v\equiv\begin{pmatrix} S_1\\ \vdots\\ S_K\end{pmatrix}, \qquad \boldsymbol{e}\equiv\begin{pmatrix} 1\\ \vdots\\ 1\end{pmatrix}, \qquad \chi_v\equiv\begin{pmatrix}\chi(S_1)\\ \vdots\\ \chi(S_K)\end{pmatrix}. \tag{1.17}$$

By multiplying the first equation in (1.16) by $\boldsymbol{e}^t$, and then using the expression for $\boldsymbol{e}^t S_v$ in (1.16), we can obtain u_c

as

$$u_c = -\frac{1}{2\pi K\nu}\left[\frac{a|\Omega|}{2\pi\sqrt{D}} + 2\pi\nu \boldsymbol{e}^t\mathcal{G}S_v + \nu \boldsymbol{e}^t\chi_v\right]. \tag{1.18}$$

By using this expression in the first equation in (1.16), we can eliminate u_c to get an equation solely for S_v.

Corollary: *The nonlinear algebraic system in (1.15) can be decoupled into an equation for S_v given by*

$$S_v + \nu\,(I-\mathcal{E})\,(\chi_v + 2\pi\mathcal{G}S_v) = \frac{a|\Omega|}{2\pi K\sqrt{D}}\,\boldsymbol{e}\,, \qquad \mathcal{E}\equiv\frac{1}{K}\boldsymbol{e}\boldsymbol{e}^t\,. \tag{1.19}$$

In terms of S_v, the constant u_c in (1.13) is given in (1.18).

The following condition on the Green's matrix $\mathcal{G}$, which reflects both the symmetry of Ω and of the configuration of the spot locations $x_1,\ldots,x_K$, gives a necessary condition for the K spots to have a common source strength S_c:

Corollary: *Suppose that $\boldsymbol{e}=(1,\ldots,1)^t$ is an eigenvector of $\mathcal{G}$, so that*

$$\mathcal{G}\boldsymbol{e} = \frac{p}{K}\boldsymbol{e}\,, \qquad p = p(x_1,\ldots,x_K)\equiv\sum_{i=1}^{K}\sum_{j=1}^{K}\mathcal{G}_{ij}\,. \tag{1.20}$$

Then, there is a solution to the NAS where $S_v = S_c\boldsymbol{e}$. The common (scalar) spot source strength S_c and the constant u_c are given explicitly by

$$S_c \equiv \frac{a|\Omega|}{2\pi K\sqrt{D}}\,, \qquad u_c = -\frac{a|\Omega|}{4\pi^2 K\nu\sqrt{D}} - \frac{S_c p}{K} - \frac{\chi(S_c)}{2\pi}\,. \tag{1.21}$$

This result readily follows as a result of the fact that $(I-\mathcal{E})\boldsymbol{e}=0$.

An example of such a special spatial configuration of spots is when K spots are equidistantly spaced on a ring of radius r_0 that is concentric with the unit disk.

Finally, for $\nu\equiv -1/\log\varepsilon \ll 1$, and for arbitrary spot locations $x_1,\ldots,x_K$, we can readily derive the following two-term expansion for S_v and u_c from (1.19) and (1.18) in terms of S_c, $\mathcal{G}$ and p:

$$S_v \sim S_c\boldsymbol{e} - 2\pi\nu S_c\left(\mathcal{G}-\frac{p}{K}I\right)\boldsymbol{e} + \mathcal{O}(\nu^2)\,; \qquad u_c \sim -\frac{a|\Omega|}{4\pi^2 K\nu\sqrt{D}} - \frac{S_c p}{K} - \frac{\chi(S_c)}{2\pi} + \mathcal{O}(\nu)\,. \tag{1.22}$$

Again here we used have the fact that $(I-\mathcal{E})\boldsymbol{e}=0$.

A detailed study of (1.15) and other aspects of localized pattern formation, including self-replicating spot patterns, is studied in [**2**]. We will focus on two aspects: the slow dynamics of spot patterns, and the stability of the spot pattern to shape deformations near the j-th spot.

1.1 Slow Spot Dynamics

Assuming that this quasi-equilibrium solution is linearly stable on an $\mathcal{O}(1)$ time-scale, we can proceed as in §2 of [**2**] to derive an ODE system for the slow evolution of the spots x_j for $j=1,\ldots,K$. The question of linear stability of the pattern must be analyzed in detail from a separate analysis.

To derive the slow ODE dynamics, we must go beyond the infinite order expansion in ν and capture the effect of the transcendentally small term that is beyond all logarithmic orders. As such, in the inner region near $x=x_j$ we

expand the solution to (1.1) as

$$u = \frac{1}{\sqrt{D}}\left(U_j(\rho) + \varepsilon U_{1j}(y) + \cdots\right), \qquad v = \sqrt{D}\left(V_j(\rho) + \varepsilon V_{1j}(y) + \cdots\right), \qquad y = \varepsilon^{-1}\left[x - x_j(\tau)\right], \quad \tau = \varepsilon^2 t\,. \tag{1.23}$$

Here $U_j(\rho)$ and $V_j(\rho)$, with $\rho = |y|$, are the radial symmetric solutions of the core problem (1.7).

We first calculate that

$$\partial_t V_j\left[\varepsilon^{-1}|x - x_j(\varepsilon^2 t)|\right] = \nabla y V_j \cdot \partial_t y = -\varepsilon^{-1} V_j'(\rho) e_\theta \cdot x_j'\,,$$

where the prime on x_j denotes derivative with respect to τ and $e_\theta \equiv (\cos\theta, \sin\theta)^T$. We then substitute (1.23) into (1.1), collect terms of order $\mathcal{O}(\varepsilon)$, and use the relation above, to derive that V_{1j} and U_{1j} for each $j = 1, \ldots, K$ satisfies

$$\mathcal{L}W_{1j} \equiv \Delta_y W_{1j} + \mathcal{M}_j W_{1j} = f_j\,, \qquad y \in \mathbb{R}^2\,, \tag{1.24 a}$$

where $y = \rho e_\theta$, and the vectors W_{1j}, f_j, and the 2×2 matrix $\mathcal{M}_j$ are defined by

$$W_{1j} \equiv \begin{pmatrix} V_{1j} \\ U_{1j} \end{pmatrix}, \qquad f \equiv \begin{pmatrix} -V_j' x_j' \cdot e_\theta \\ 0 \end{pmatrix}, \qquad \mathcal{M}_j \equiv \begin{pmatrix} -1 + 2U_j V_j & V_j^2 \\ -2U_j V_j & -V_j^2 \end{pmatrix}. \tag{1.24 b}$$

Next, we derive the required far-field condition for W_{1j} as $|y| \to \infty$ that results from performing a higher order matching of the outer and inner solutions. By performing the Taylor series expansion of the solution to (1.13), and then matching to the inner solution, we we obtain that the solution to (1.24) must satisfy

$$W_{1j} \sim \begin{pmatrix} 0 \\ \alpha_j \cdot y \end{pmatrix} \quad \text{as} \quad y_j \to \infty\,, \qquad \alpha_j \equiv -2\pi S_j \nabla R(x_j; x_j) - 2\pi \sum_{\substack{j=1 \\ j\neq i}}^{N} S_i \nabla G(x_j; x_i)\,. \tag{1.25}$$

The problem (1.24), subject to (1.25), will determine x_j' in terms of the vector α_j.

We observe that $\mathcal{L}W_{1j}$ is not self-adjoint, since $\mathcal{M}_j$ is not a symmetric matrix. It does, however, have a nontrivial nullspace. To see this, we differentiate the core problem (1.7) with respect to ρ. It readily follows that there are two independent nontrivial solution to the homogeneous problem $LW_{1j} = 0$ given by $W_{1j} = \left(V_j', U_j'\right)^T \cos\theta$ and $W_{1j} = \left(V_j', U_j'\right)^T \sin\theta$. As such, there must exist two nontrivial solutions to the homogeneous adjoint problem $L^\star \Psi^\star = 0$. This means that there must be a solvability condition for the existence of a solution to (1.24). This condition, determines x_j'. The definition of the adjoint operator and the derivation of the solvability condition is given in the next result.

Lemmma: *A necessary condition for the existence of a solution of (1.24), subject to the far-field condition (1.25), is that*

$$x_j' = \gamma(S_j)\alpha\,, \qquad \gamma \equiv \gamma(S) = \frac{-2}{\int_0^\infty \rho V_j'(\rho)\hat{\Phi}^*(\rho)\,d\rho}\,. \tag{1.26}$$

Here $V(\rho)$ satisfies the core problem (1.7) at the given value of S_j, and $\hat{\Phi}^*(\rho)$ is the first component of the radially symmetric adjoint solution $\hat{P}^*(\rho) \equiv \left(\hat{\Phi}^*(\rho), \hat{\Psi}^*(\rho)\right)^T$ satisfying

$$\Delta_\rho \hat{P}^* + \mathcal{M}_0^T \hat{P}^* = \mathbf{0}\,, \qquad 0 < \rho < \infty\,, \tag{1.27}$$

subject to the far-field conditions that $\hat{\Phi}^* \to 0$ *exponentially as* $\rho \to \infty$ *and that* $\hat{\Psi}^* \sim 1/\rho$ *as* $\rho \to \infty$. *Here* $\mathcal{M}_0^T$ *denotes the transpose of the matrix* $\mathcal{M}_0$ *in (1.24 b) and* $\Delta_\rho \hat{P}^* \equiv \partial_{\rho\rho}\hat{P}^* + \rho^{-1}\partial_\rho \hat{P}^* - \rho^{-2}\hat{P}^*$.

Proof: We now derive this result. We begin by writing the homogeneous adjoint problem to (1.24 *a*) as

$$\Delta_y p + \mathcal{M}_0^T p = 0\,, \qquad y \in \mathbb{R}^2\,, \qquad p \equiv \begin{pmatrix} \Phi^* \\ \Psi^* \end{pmatrix}. \tag{1.28}$$

We seek solutions to this problem as either $P_c^* \equiv \hat{P}^* \cos\theta$ or $P_s^* \equiv \hat{P}^* \sin\theta$, where $\hat{P}^*$ satisfies the radially symmetric problem (1.27). We write the two-component vector $\hat{P}^*$ as $\hat{P}^* = (\hat{\Phi}^*, \hat{\Psi}^*)^T$ and we impose the asymptotic boundary conditions $\hat{\Phi}^* \to 0$ exponentially as $\rho \to \infty$ and the normalization condition that $\hat{\Psi}^* \sim \rho^{-1}$ as $\rho \to \infty$.

Next, we apply a solvability condition to the solution of (1.24) with (1.25) by applying Green's identity over a large ball B_σ of radius $\sigma \gg 1$ centered at $y = 0$. Upon using Green's identity to P_c^* and W_1 we derive

$$\lim_{\sigma\to\infty} \int_{B_\sigma} \left[(P_c^*)^T \left(\Delta_y W_1 + \mathcal{M}_0 W_1\right) - (W_1)^T \left(\Delta_y P_c^* + \mathcal{M}_0^T P_c^*\right)\right] dy$$
$$= \lim_{\sigma\to\infty} \int_{\partial B_\sigma} \left[(P_c^*)^T \partial_\rho W_1 - {W_1}^T \partial_\rho P_c^* \right]\Big|_{\rho=\sigma} dy\,. \tag{1.29}$$

Then, upon using (1.24), together with the asymptotic boundary conditions for W_1 in (1.25) and for P_c^*, we obtain that (1.29) reduces to

$$-x_{j1}' \int_0^{2\pi}\int_0^\infty \hat{\Phi}^* V' \cos^2\theta\, \rho\, d\rho\, d\theta = \lim_{\sigma\to\infty} \int_0^{2\pi} \left(\left(\frac{\cos\theta}{\rho}\right)\alpha_1 \cos\theta - \alpha_1 \rho \cos\theta \left(\frac{-1}{\rho^2}\right)\cos\theta \right)\Big|_{\rho=\sigma} \sigma\, d\theta\,, \tag{1.30}$$

where x_{j1} and α_1 are the first components of x_j and α, respectively. Therefore, $x_{j1}' \int_0^\infty \rho V' \hat{\Phi}^*\, d\rho = -2\alpha_1$, which is the first component of (1.26). The second component of (1.26) follows by repeating this calculation with P_s^*. ■

Numerical computations of $\gamma(S_j)$ in [**2**], show that $\gamma(S_j) > 0$ on $0 < Sj < 5.5$. By using this lemma, we obtain the following main result for the dynamics of a K-spot quasi-equilibrium solution, as was obtained in [**2**].

Principal Result: *For* $\varepsilon \to 0$ *the slow dynamics of a collection* $x_1, \ldots, x_K$ *of spots satisfies the differential-algebraic system (DAE),*

$$x_j' \sim -2\pi\varepsilon^2 \gamma(S_j) \left(S_j \nabla R(x_j; x_j) + \sum_{\substack{j=1 \\ j\neq i}}^{N} S_i \nabla G(x_j; x_i) \right), \qquad j = 1, \ldots, K\,. \tag{1.31}$$

Here the source strengths S_j, *for* $j = 1, \ldots, K$, *are determined in terms of* $x_1, \ldots, x_K$ *by the nonlinear algebraic system (1.15). The function* $\gamma(S_j)$ *is a certain positive function determined in terms of a solvability condition.*

1.2 Linear Stability of the Spot Profile

Next, we study the stability of the quasi-equilibrium one-spot solution constructed above to instabilities occurring on a fast $\mathcal{O}(1)$ time-scale. Since the speed of the slow drift of the spots in (1.31) is $\mathcal{O}(\varepsilon^2) \ll 1$, in our stability analysis we will assume that the spot is asymptotically stationary. We begin the stability analysis by letting u_e and v_e denote the quasi-equilibrium solution, and we introduce the perturbation

$$u = u_e + \mathrm{e}^{\lambda t}\eta\,, \qquad v = v_e + \mathrm{e}^{\lambda t}\phi\,. \tag{1.32}$$

m	Σ_m
2	4.303
3	5.439
4	6.143
5	6.403
6	6.517

Table 1. Numerical results computed from (1.35) for the threshold values of S, denoted by Σ_m, as a function of the integer angular mode m where an instability first occurs for the core problem (1.7) as S increases.

By substituting (1.32) into (1.1) and linearizing, we obtain the following eigenvalue problem for ϕ and η:

$$\varepsilon^2\Delta\phi-\phi+2u_ev_e\phi+v_e^2\eta=\lambda\phi\,,\quad D\Delta\eta-2\varepsilon^{-2}u_ev_e\phi-\varepsilon^{-2}v_e^2\eta=\varepsilon^2\lambda\eta\,,\quad x\in\Omega\,;\quad \partial_n\phi=\partial_n\eta=0\,,\quad x\in\partial\Omega\,. \tag{1.33}$$

In the inner region near x_j we look for an $\mathcal{O}(1)$ time-scale instability associated with the local angular integer mode m by introducing the new variables $N(\rho)$ and $\Phi(\rho)$ by

$$\eta=\frac{1}{D}e^{im\theta}N(\rho)\,,\qquad \phi=e^{im\theta}\Phi(\rho)\,,\qquad \rho=|y|\,,\qquad y=\varepsilon^{-1}(x-x_j)\,, \tag{1.34}$$

where $y^t=\rho(\cos\theta,\sin\theta)$. Substituting (1.34) into (1.33), and by using $u_e\sim D^{-1/2}U(\rho)$ and $v_e\sim\sqrt{D}V(\rho)$, where U and V satisfy the core problem (1.7), we obtain the following radially symmetric eigenvalue problem:

$$\mathcal{L}_m\Phi-\Phi+2UV\Phi+V^2N=\lambda\Phi\,,\qquad \mathcal{L}_mN-2UV\Phi-V^2N=0\,,\qquad 0\le\rho<\infty\,. \tag{1.35}$$

Here $\mathcal{L}_m\Phi\equiv\partial_{\rho\rho}\Phi+\rho^{-1}\partial_\rho\Phi-m^2\rho^{-2}\Phi$. We impose the usual regularity condition for Φ and N at $\rho=0$. As we show below, the appropriate far-field boundary conditions for (1.35) as $\rho\to\infty$ depends on whether $m=0$ or $m\ge2$.

The eigenvalue problem (1.35) does not appear to be amenable to analysis, and thus we solve it numerically for various integer values of m. We denote λ_0 to be the eigenvalue of (1.35) with the largest real part. Since U and V depend on S from (1.7), we have implicitly that $\lambda_0=\lambda_0(S,m)$. To determine the onset of any instabilities, we compute any threshold values $S=\Sigma_m$ where $\mathrm{Re}(\lambda_0(\Sigma_m,m))=0$. In our computations, we only consider $m=0,2,3,4,\ldots$, since $\lambda_0=0$ for any value of S for the translational mode $m=1$. A higher order perturbation analysis for the $m=1$ mode generates only weak instabilities occurring on an asymptotically long $\mathcal{O}(\varepsilon^{-2})$ time-scale. Any such instabilities are reflected in instabilities in the ODE (1.31).

When $m\ge2$ we can impose the asymptotic decay conditions that Φ decays exponentially as $\rho\to\infty$ while $N\sim\mathcal{O}(\rho^{-m})\to0$ as $\rho\to\infty$. With these conditions (1.35) is discretized with centered differences on a large but finite domain. We then determine $\lambda_0(S,m)$ by computing the eigenvalues of a matrix eigenvalue problem. For $m\ge2$ our computations show that $\lambda_0(S,m)$ is real and that $\lambda_0(S,m)>0$ when $S>\Sigma_m$. The threshold value Σ_m is tabulated in Table 1 for $m=2,\ldots,6$. In our computations we took 300 meshpoints on the interval $0\le\rho<20$. To the number of significant digits shown in Table 1, the results there are insensitive to increasing either the domain length or the number of grid points. It follows from Table 1 that the smallest value of S where an instability is triggered occurs for the "peanut-splitting" instability $m=2$ at the threshold value $S=\Sigma_2\approx4.3$. In Fig. 2(a) we plot $\lambda_0(S,m)$ as a function of S for $m=2$, $m=3$ and $m=4$.

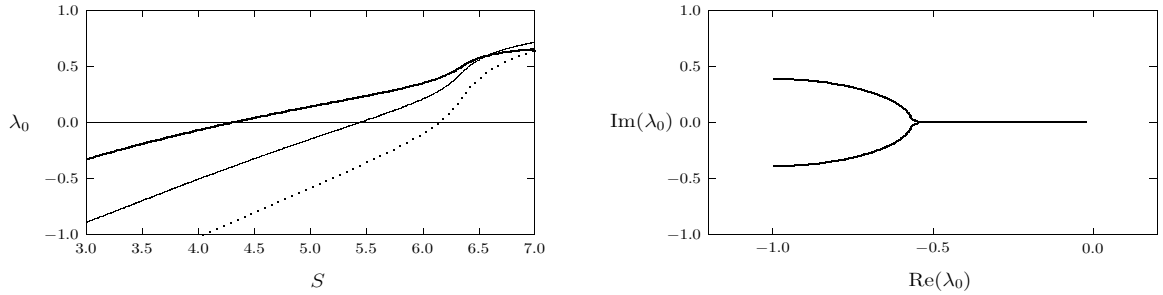

(a) λ_0 vs. S for $m = 2, 3, 4$

(b) $\mathrm{Im}(\lambda_0)$ and $\mathrm{Re}(\lambda_0)$ for $m = 0$

FIGURE 2. Left figure: Plot of the largest (real) eigenvalue $\lambda_0(S, m)$ of (1.35) vs. S for $m = 2$ (heavy solid), $m = 3$ (solid), and $m = 4$ (dotted). Right figure: Plot in the complex plane of the path of the eigenvalue $\lambda_0(S, 0)$ of largest real part of (1.35) with $m = 0$ and $2.8 < S < 7.5$. For $S < 2.8$, $\lambda_0 \approx -1.0$ and arises from the discretization of the continuous spectrum (not shown). For $2.8 < S < 4.98$, $\lambda_0(S, 0)$ occurs as a complex conjugate pair which monotonically approaches the real axis as S increases. This pair merges onto the real axis at $S \approx 4.79$. As S increases further, $\lambda_0(S, 0)$ remains real but negative.

By extending this result to the K-spot case, the following result characterizing spot-splitting was obtained in [**2**].

Spot-Splitting Criterion: *Let $D = \mathcal{O}(1)$ and $\varepsilon \to 0$ and consider a K-spot quasi-equilibrium solution to (1.1). Let S_j for $j = 1, \ldots, K$, satisfy the nonlinear algebraic system (1.15) when $K > 1$. For $K \geq 1$ the quasi-equilibrium solution is stable with respect to the other local angular modes $m = 2, 3, 4, \ldots$ provided that $S_j < \Sigma_2 \approx 4.303$ for all $j = 1, \ldots, K$. The J^{th} spot will become unstable to the $m = 2$ mode if S_J exceeds the threshold value Σ_2. This peanut-splitting instability from the linearized problem is found to initiate a nonlinear spot self-replication process.*

Numerical confirmation of this theory was shown in [**2**], and will be illustrated in class.

As a final remark, there are two other instability mechanisms that are associated with locally radially symmetric solutions (i.e. the $m = 0$ mode) near the spot. The key issue is that for the $m = 0$ mode, we have that N grows logarithmically at infinity, which effectively coupled all the spots together. This eigenvalue problem was derived and analzyed in [**2**].

References

[1] P. W. Davis, P. Blanchedeau, E. Dullos, P. De Kepper, *Dividing Blobs, Chemical Flowers, and Patterned Islands in a Reaction-Diffusion System*, J. Phys. Chem. A, **102**, No. 43, (1998), pp. 8236–8244.

[2] T. Kolokolnikov, M. J. Ward, J. Wei, *Spot Self-Replication and Dynamics for the Schnakenburg Model in a Two-Dimensional Domain*, J. Nonlinear Sci., **19**(1), (2009), pp. 1–56.

[3] K. J. Lee, W. D. McCormick, J. E. Pearson, H. L. Swinney, *Experimental Observation of Self-Replicating Spots in a Reaction-Diffusion System*, Nature, **369**, (1994), pp. 215-218.

[4] J. E. Pearson, *Complex Patterns in a Simple System*, Science, **216**, (1993), pp. 189–192.

[5] V. K. Vanag, I. R. Epstein, *Localized Patterns in Reaction-Diffusion Systems*, Chaos **17**, No. 3, 037110, (2007).